JACS
JOURNAL OF THE AMERICAN CHEMICAL SOCIETY
Article
pubs.acs.org/JACS

Detection of α-Synuclein Amyloidogenic Aggregates *in Vitro* and in Cells using Light-Switching Dipyridophenazine Ruthenium(II) Complexes

Nathan P. Cook,[†,⊥] Kiri Kilpatrick,[‡,⊥] Laura Segatori,*[,‡,§,#] and Angel A. Martí*[,†,§]

[†]Departments of Chemistry, [‡]Chemical and Biomolecular Engineering, [§]Bioengineering, and [#]Biochemistry and Cell Biology, Rice University, Houston Texas 77005, United States

Supporting Information

ABSTRACT: Protein aggregation is the hallmark of a number of neurodegenerative diseases including Parkinson's and Huntington's diseases. There is a significant interest in understanding the molecular mechanisms involved in the self-association and fibrillization of monomeric soluble proteins into insoluble deposits *in vivo* and *in vitro*. Probes with novel properties, such as red-shifted emission, large Stokes shifts, and high photostability, are desirable for a variety of protein aggregation studies. To respond to the increasing need for aggregation−responsive compounds suitable to cellular studies, we present a ruthenium(II) dipyridophenazine derivative, $[Ru(phen)_2dppz]^{2+}$ (phen =1,10-phenanthroline, dppz = dipyrido[3,2-a:2′.3′-c]phenazine), to study aggregation of α-synuclein (αS), which is associated with the development of Parkinson's disease. We demonstrated the use of $[Ru(phen)_2dppz]^{2+}$ to monitor αS fibril formation in real-time and to detect and quantify αS aggregates in neuroglioma cells, thereby providing a novel molecular tool to study protein deposition diseases *in vitro* and *in vivo*.

INTRODUCTION

Parkinson's disease (PD) is the most prevalent neurodegenerative movement disorder. It is characterized by the accumulation of proteinaceous cytoplasmic inclusions (Lewy bodies) in dopaminergic neurons.[1] The major component of Lewy bodies is α-synuclein (αS),[2] a natively unfolded 140 amino acid protein with high propensity to misfold and aggregate.[3] The role of αS in the development of PD has been extensively investigated and evidence points to a correlation between αS misfolding and aggregation and the progression of PD pathogenesis.[4−6] However, the molecular mechanisms underlying αS misfolding and aggregation and the role of αS inclusions in the development of PD remain elusive.

Currently available techniques to monitor the accumulation of protein aggregates in cell cultures present a number of limitations. Analytical methods, including transmission electron microscopy and polyacrylamide gel electrophoresis followed by Western blotting,[7] are time-consuming and not amenable to high-throughput applications. Fluorescence-based techniques have been widely used to monitor αS aggregation *in vitro* and *in vivo* and are typically based on the fusion of αS to reporter proteins, such as the green fluorescent protein (GFP),[8] or covalent binding of αS to small fluorophores, such as biarsenical labeling reagents[9] and Alexa dyes.[10] To avoid altering the peptide backbone of the target protein or inducing covalent modifications that could potentially influence its folding landscape, significant focus has been devoted to the design of compounds that display high affinity for specific protein conformations, such as the fibrillar aggregates characteristic of amyloidogenic proteins. Thioflavin T (ThT), a benzothiazole molecule that displays minimal fluorescence in aqueous media and enhanced fluorescence when bound to amyloid aggregates, has been extensively used to probe and quantify fibril formation.[11,12] Particularly, ThT has been used to characterize the structure of αS fibrils and to investigate the aggregation kinetics of different αS mutants *in vitro*,[13,14] which is crucial to elucidate the molecular mechanisms of PD pathogenesis.

The main drawbacks associated with the use of ThT to detect protein aggregates in cells are its small Stokes shift and green fluorescence emission, which overlaps with intrinsic fluorescence properties of other cellular components, such as flavins or reduced NAD(P)H.[15] Aldehyde-containing reagents typically used to fix cell and tissue samples generate an autofluorescent background signal with spectral properties similar to ThT.[16] Furthermore, polyphenols, such as curcumin and quercetin, which inhibit aggregation *in vitro*, present strong absorptive and fluorescent properties that overlap with ThT photoluminescence and may compete with ThT for binding to fibrillar binding sites.[17] In summary, there is an urgent need for fibrillization responsive probes with large Stokes shifts and red-shifted fluorescence emissions, which display low background signal and could be used as alternatives to ThT when other commonly used green fluorescent reporters are present. The development of tools to monitor cellular aggregation of proteins, in turn, will provide new avenues to study the cellular pathogenesis of numerous human diseases that result from deposition of proteinaceous aggregates.[18]

In this work, we demonstrate the use of the dipyridophenazine derivative, $[Ru(phen)_2dppz]^{2+}$ (phen =1,10-phenanthroline, dppz = dipyrido[3,2-a:2′.3′-c]phenazine), to monitor the formation of αS fibrils *in vitro* and to detect αS aggregation in cell cultures. $[Ru(phen)_2dppz]^{2+}$ and related compounds are commonly referred to as "light switch molecules" because of their on−off photoluminescent behavior. These complexes are generally nonemissive in aqueous solution. However, in the

Received: October 10, 2012
Published: December 14, 2012

   dx.doi.org/10.1021/ja3100287 | J. Am. Chem. Soc. 2012, 134, 20776−20782

presence of biomolecules, such as DNA, which have a fibril-like structure, they display a dramatic increase in photoluminescence intensity.[19] We previously reported the use of the dipyridophenazine probe $[Ru(bpy)_2dppz]^{2+}$ (bpy =2,2′-bipyridine; dppz = dipyrido[3,2-a:2′.3′-c]phenazine) for real-time monitoring of Aβ aggregation *in vitro*.[20] These complexes have been used in a wide variety of applications including DNA detection,[21] photoinduced electron transport,[22] carbon nanotubes,[23] and cell imaging.[24,25] To the best of our knowledge, while ruthenium(II) complexes and related metal complexes have been extensively studied in cells,[26−28] they have never been used to characterize αS fibrilization or to measure intracellular protein aggregation. We demonstrate here the use of the metal complex $[Ru(phen)_2dppz]^{2+}$, which presents light switching properties and a significantly stronger photoluminescence intensity than $[Ru(bpy)_2dppz]^{2+}$,[29] as a real-time probe for αS fibrillization. Furthermore, we investigated the use of $[Ru(phen)_2dppz]^{2+}$ complexes to detect αS aggregation in human neuroglioma cells that overexpress αS fused to GFP and accumulate αS-GFP aggregates. We observed an increase in $[Ru(phen)_2dppz]^{2+}$ photoluminescence under conditions that induce protein aggregation, such as inhibition of proteasomal degradation. We also demonstrated colocalization of αS-GFP and $[Ru(phen)_2dppz]^{2+}$ photoluminescence in cells, indicating a correlation between the intensity of $[Ru(phen)_2dppz]^{2+}$ photoluminescence and the formation of αS aggregates. In summary, we demonstrated the use of $[Ru(phen)_2dppz]^{2+}$ as a molecular probe to detect αS aggregation *in vitro* and in cells, thereby providing a novel and much needed tool to quantify the aggregation of amyloidogenic proteins and to study the cellular pathogenesis of protein deposition diseases.

EXPERIMENTAL SECTION

Synthesis of Ruthenium(II) Complexes. *cis-Ru(phen)$_2$Cl$_2$.* This complex is synthesized following Sullivan et al.[30] In a typical synthesis, $RuCl_3{\cdot}xH_2O$ (56 mmol, Strem chemicals), phen (112 mmol, Sigma-Aldrich), and LiCl (3.7 mmol, VWR) were refluxed in 25 mL DMF for 8 h.[30] Acetone was then added to the reaction mixture, which was cooled overnight at 4 °C. The resulting complex was used without further purification.

cis-Ru(bpy)$_2$Cl$_2$. *cis*-$Ru(bpy)_2Cl_2$ was purchased from Strem chemicals and used as received.

Dipyrido[3,2-a:2′.3′-c]phenazine (dppz). The dppz ligand was synthesized in two parts, following Dickeson et al.[31] 1,10-phenanthroline-5,6-dione was synthesized by adding an ice cold mixture of H_2SO_4 (10 mL) and HNO_3 (5 mL) to 1g of phen and 1g KBr. The reaction was refluxed for 3 h, poured onto crushed ice, then carefully neutralized with NaOH to slightly acidic pH and extracted with dichloromethane. The 1,10-phenanthroline-5,6-dione (1.42 mmol) was subsequently reacted with diaminobenzene (1.71 mmol) in 30 mL of ethanol for 2 h under reflux.[31]

[Ru(phen)$_2$dppz]$^{2+}$. *cis*-$Ru(phen)_2Cl_2{\cdot}2H_2O$ was refluxed in 1:1 methanol and water with vigorous stirring for 3 h with dppz as described by Amouyal et al.[32] Upon cooling, the product was precipitated from solution by the addition of NH_4PF_6 and filtered. The reddish-orange crystals were purified by column chromatography (4:1 dichloromethane and acetonitrile) and recrystallization (90:10 ethanol and water). An extinction coefficient of 20 000 M^{-1} cm^{-1} at 440 nm was used to adjust the compound concentration.[33]

[Ru(bpy)$_2$dppz]$^{2+}$. This complex was synthesized and purified following the procedure described above with the exception that *cis*-$Ru(bpy)_2Cl_2$ was used as starting reagent. An extinction coefficient of 15 700 M^{-1} cm^{-1} at 448 nm was used to verify the compound concentrations.[32]

***In vitro* Aggregation Experiments.** The αS fibrils were prepared as described by Antony et al.[11] Briefly, a 100 μM solution of αS (rPeptide) was prepared in PBS (pH 7.4, 300 mM NaCl, 100 mM sodium phosphate). The concentration was verified using an extinction coefficient of 5600 $L{\cdot}M^{-1}$ cm^{-1}. Spermine was then added to a final concentration of 100 μM, and the solution was incubated with 10 μM $[Ru(phen)_2dppz]^{2+}$ or $[Ru(bpy)_2dppz]^{2+}$ in glass vials. Fibrillization reactions were incubated at 37 °C and stirred at 550 rpm, and photoluminescence spectra taken every 30 min with a Horiba-Jobin Yvon Fluorolog 3. $[Ru(phen)_2dppz]^{2+}$ and $[Ru(bpy)_2dppz]^{2+}$ were excited at 440 nm, and front face emission was measured from 550 to 700 nm with 2 nm slits. Both emission and excitation were corrected for instrument-dependent inefficiencies. The solution photoluminescence intensity at 640 nm was monitored to quantify the monomer to fibril transition. The photoluminescence intensity of 10 μM $[Ru(phen)_2dppz]^{2+}$ and $[Ru(bpy)_2dppz]^{2+}$ solutions in PBS was used as blanks.

AFM samples were prepared by dropping 20 μL of αS solution onto a freshly cleaved mica surface. The protein was allowed to adhere to the mica for 5 min then washed with 20 μL H_2O three times while being spun dry for 10 min. At 1.0 Hz, 5 × 5 μm scans were taken with 512 lines of resolution. TEM samples were prepared by dropping 10 μL of αS solution onto a glow discharged 200 mesh carbon type B coated copper grid (Ted Pella 01811). The fibrils were allowed to adhere for 5 min, then buffer solution was wicked away with filter paper. The grid was washed 3 times with 10 μL H_2O and stained with 10 μL of a 2% w/v phosphotungstic acid solution for 30 s. Samples were imaged on a JEOL 2010 transmission electron microscope operating at 100 kV.

Aggregation Studies in Cell Cultures. The cDNA encoding human wild-type α-syn (P37840) was generated by assembly PCR. The PCR product was first cloned into pENTR11 and then transferred into pcDNA6.2/C-EmGFP-DEST using Gateway recombination cloning technology (Invitrogen) according to the manufacture's protocol. Human H4 neuroglioma cells (HTB-148, ATCC) were cultured in high glucose DMEM (Fisher) supplemented with 10% fetal bovine serum, 1% PSQ, 4 mM L-Glutamine, and 1 mM sodium pyruvate and maintained at 37 °C and 5% CO_2. Cells were transfected with pcDNA6.2/α-syn-EmGFP using lipofectamine 2000 according to the manufacturer's instructions (Invitrogen). Stably transfected cells were selected by culturing cells with 5 μg/mL blasticidin S HCl, and monoclonal populations of blasticidin-resistant cells were isolated.

H4 and H4/α-syn-GFP cells were cultured on poly L-lysine (Sigma) coated glass coverslips and treated with MG-132 (2 μM) for 16 h at 37 °C. After treatment with MG-132, cells were fixed for 30 min using 4% paraformaldehyde, permeabilized for 30 min on ice with 0.5% Triton X-100, and incubated for 30 min with $[Ru(phen)_2dppz]^{2+}$ or with the ProteoStat Aggregation detection dye (Enzo Life Sciences) according to the manufacturer's protocol.

Protein aggregation in H4/α-syn-GFP cells was analyzed by fluorescence microscopy (Olympus Fluoview 1000) using a 458-nm laser and 560−660 nm band-pass filter to detect $[Ru(phen)_2dppz]^{2+}$ photoluminescence. Colocalization of αS-GFP and $[Ru(phen)_2dppz]^{2+}$ in H4/α-syn-GFP cells was evaluated using the Colocalization Colormap script, an ImageJ plugin that calculates the correlation of intensity between complementary fluorescent signals. The results are presented as a colormap, where hot colors represent positive correlation and cold colors represent negative correlation.[34] Colormaps were analyzed using the ImageJ plugin Threshold Color, which allows RGB images to be filtered based on hue, saturation, and brightness (http://www.dentistry.bham.ac.uk/landinig/software/software.html). To indicate high colocalization, the hue was filtered to display pixel intensities from 0 to 35 and designated as red pixels. To indicate low colocalization, the hue was filtered to display pixel intensities from 35 to 60 and designated as yellow pixels. Pixels in the hue range from 60 to 255 were considered negative correlation and not evaluated in this study. To quantify aggregation in H4 and H4/α-syn-GFP cells, the average pixel intensity of images from cells stained with aggregate dye was evaluated by determining the brightness of

dx.doi.org/10.1021/ja3100287 | J. Am. Chem. Soc. 2012, 134, 20776−20782

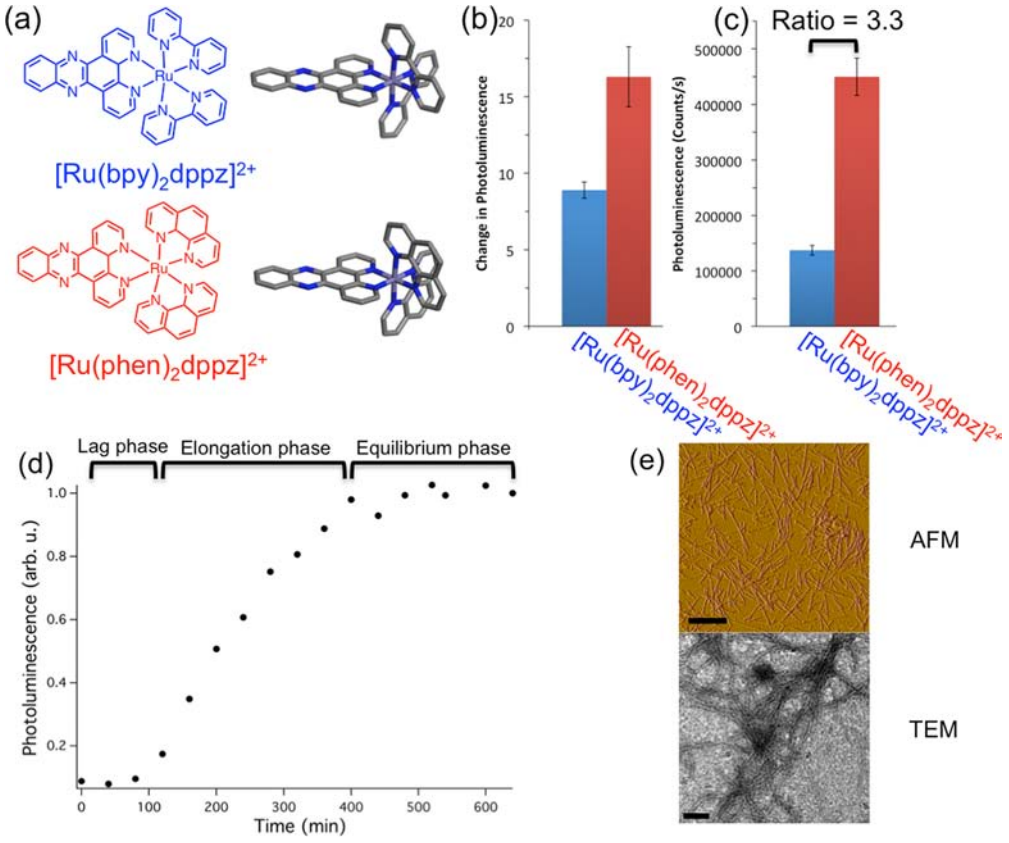

Figure 1. Detection of αS fibrillization using $[Ru(phen)_2dppz]^{2+}$. (a) Schematic (left) and 3-D (right) structures of $[Ru(bpy)_2dppz]^{2+}$ and $[Ru(phen)_2dppz]^{2+}$ (hydrogen atoms have been omitted for clarity). (b) Change in photoluminescence intensity of $[Ru(bpy)_2dppz]^{2+}$ (blue) and $[Ru(phen)_2dppz]^{2+}$ (red) in the presence of αS upon transition from monomeric to fibrillar state. (c) Comparison of the absolute photoluminescence intensity of $[Ru(bpy)_2dppz]^{2+}$ (blue) and $[Ru(phen)_2dppz]^{2+}$ (red) in the presence of aggregated αS. (d) Fibrillization of αS in real-time detected by monitoring $[Ru(phen)_2dppz]^{2+}$ photoluminescence (λ_{em} = 640 nm). (e) AFM (top) and TEM (bottom) of mature αS fibrils (scale bars AFM: 1 μm; TEM = 200 nm). The experiments were performed in PBS (pH 7.4, 300 mM NaCl, 100 mM sodium phosphate), with 100 μM αS, 100 μM spermine, and 10 μM of the ruthenium complex.

each pixel on a scale of 0−255, where 0 is black and 255 is white, and calculating the average pixel brightness across the entire image.

Protein aggregation was evaluated by measuring fluorescence intensity by flow cytometry (FACSCanto II, BD Biosciences) using a 488 nm argon laser and 585/42 band-pass filter. H4 and H4/α-syn-GFP cells were treated with MG-132 and incubated with $[Ru(phen)_2dppz]^{2+}$ or the ProteoStat dye as described above. The aggregation propensity factor (APF) was calculated using the following formula: $APF = 100 \times (MFI_{treated} - MFI_{control})/MFI_{treated}$, where MFI is the mean fluorescence intensity of the aggregation dye and untreated H4 cells were used as the control.

RESULTS AND DISCUSSION

Real-Time Detection of the Formation of αS Fibrillar Aggregates. Most amyloid responsive ligands, such as ThT, are widely used to monitor fibril formation in real-time but are of limited utility for the detection of protein aggregates in cell cultures and *in vivo*. In an attempt to develop a reliable molecular probe to assess protein aggregation in cells, we investigated the use of ruthenium(II) dipyridophenazine complexes to monitor the fibrillization and intracellular aggregation of αS, a misfolding- and aggregation-prone protein associated with the development of PD.[35] We previously reported that $[Ru(bpy)_2dppz]^{2+}$ (Figure 1a) presents high affinity for $A\beta_{1-40}$ fibrils and can be used to monitor in real-time the transition of $A\beta_{1-40}$ monomers into fibrils.[20] Based on this evidence, we hypothesized that ruthenium(II) dipyridophenazine derivatives can be used to detect fibrillar aggregates of other amyloidogenic proteins. To investigate this question, we monitored the photoluminescence intensity of ruthenium(II) dipyridophenazine derivatives incubated with purified αS as described previously by Antony et al.[11] We observed a 9-fold increase in $[Ru(bpy)_2dppz]^{2+}$ photoluminescence when αS transitions from monomeric to fibrillar state (Figure 1b), suggesting high affinity of this compound for amyloidogenic protein aggregates. Previous studies showed that $[Ru(phen)_2dppz]^{2+}$ presents light switching characteristics but displays stronger photoluminescence intensity (higher quantum yield) than $[Ru(bpy)_2dppz]^{2+}$ when bound to DNA.[29] Interestingly, $[Ru(bpy)_2dppz]^{2+}$ and $[Ru(phen)_2dppz]^{2+}$ have related chemical structures (Figure 1a) and similar UV−vis and photoluminescence spectra with far-red emissions at ca. 640 nm and large Stokes shifts[36] of about 190 nm (Figure S1). We observed an 18-fold increase in $[Ru(phen)_2dppz]^{2+}$ photoluminescence in the presence of fibrillar αS, which is twice the increase in photoluminescence signal obtained using $[Ru(bpy)_2dppz]^{2+}$ under the same conditions (Figure 1b). To further evaluate the use of these two metal complexes to quantify αS aggregation, we compared their absolute photoluminescence intensity. As shown in Figure 1c, the absolute photoluminescence of $[Ru(phen)_2dppz]^{2+}$ is 3.3-fold higher than that of $[Ru(bpy)_2dppz]^{2+}$ in the presence of equal concentrations of aggregated αS and obtained under the same

dx.doi.org/10.1021/ja3100287 | J. Am. Chem. Soc. 2012, 134, 20776−20782

experimental conditions. Since $[Ru(phen)_2dppz]^{2+}$ presented the largest change in photoluminescence and the strongest photoluminescence intensity, it was selected to further investigate αS aggregation.

The more intense photoluminescence of $[Ru(phen)_2dppz]^{2+}$ in the presence of fibrillar αS is in agreement with a previous study by Jenkins et al. reporting that $[Ru(phen)_2dppz]^{2+}$ photoluminescence is approximately 6 times higher than that of the bipyridine derivative when bound to DNA.[29] Interestingly, when both complexes are dissolved in acetonitrile, they display similar quantum yields.[29] Jenkins et al. hypothesized that the phenanthroline complex, being more hydrophobic, shields better the dppz ligand from water, thus explaining the superior photoluminescence properties of the phenanthroline complex compared to the bipyridine complex. In agreement with this previous report, our study suggests that the higher photoluminescence signal measured upon $[Ru(phen)_2dppz]^{2+}$ binding to fibrillar αS is due to the stronger interaction between $[Ru(phen)_2dppz]^{2+}$ and the fibrillar aggregates than the parent compound, $[Ru(bpy)_2dppz]^{2+}$. This is consistent with the availability of exposed hydrophobic domains in the fibril structure that allow stronger binding of the more hydrophobic $[Ru(phen)_2dppz]^{2+}$ compound. This binding results in a larger change in the microenvironment surrounding $[Ru(phen)_2dppz]^{2+}$, and consequently, a larger increase in photoluminescence.

A number of αS alleles presenting point mutations that alter the protein's rate of aggregation have been characterized.[37−40] Among the mutations linked to familial cases of PD, the A30P αS variant was reported to aggregate at slower rate than wild-type αS *in vitro*.[41] In agreement with these observations, we observed an 11-fold increase in the photoluminescence of $[Ru(phen)_2dppz]^{2+}$ in the presence of A30P αS fibrils under the same conditions used to test wild-type αS, confirming that $[Ru(phen)_2dppz]^{2+}$ is a reliable probe to monitor αS protein fibrillization (Figure S2). Furthermore, control studies conducted to evaluate $[Ru(phen)_2dppz]^{2+}$ photoluminescence in the presence of the globular protein bovine serum albumin (BSA) revealed minimal changes in photoluminescence signal under the same conditions used to test αS. In particular, $[Ru(phen)_2dppz]^{2+}$ photoluminescence in the presence of fibrillar αS was 8-fold higher than in the presence of BSA when equal amounts of proteins (1250 μg/mL) were tested (Figure S3).

Because $[Ru(phen)_2dppz]^{2+}$ photoluminescence is highly dependent on changes in αS aggregation state, we asked whether this probe can be used to monitor real-time formation of αS fibrils *in vitro*. A solution of monomeric αS was incubated with $[Ru(phen)_2dppz]^{2+}$, and αS aggregation was induced as previously described.[11] The complexes were excited at the metal-to-ligand charge transfer (MLCT) band (440 nm), and the emission was recorded at 640 nm (Figure S1). The photoluminescence data depict the typical sigmoidal curve (Figure 1d) observed when monitoring the formation of amyloidogenic fibrils in real-time.[42] The initial phase represents a lag phase (approximately 2 h) where αS is predominantly in a monomeric, soluble state, that is followed by an elongation phase during which fibrillization occurs exponentially and then by a plateau phase where fibrillar and monomeric αS are present in equilibrium. The presence of fibril aggregates was confirmed by AFM and TEM (Figure 1e). Furthermore, the real-time fibrillization kinetics of αS with $[Ru(phen)_2dppz]^{2+}$ are consistent with those obtained by Antony et al.[11] using ThT as probe.[43]

Detection of αS Aggregates in Neuroglioma Cells. To investigate the use of $[Ru(phen)_2dppz]^{2+}$ as a probe to monitor αS aggregation in living cells, we used human neuroglioma cells (H4) stably transfected for the overexpression of αS fused to GFP (H4/α-syn-GFP). The use of αS-GFP fusion as a reliable reporter for disease-associated phenotypes has been previously established.[44−46] To evaluate binding of $[Ru(phen)_2dppz]^{2+}$ to αS aggregates, we first quantified $[Ru(phen)_2dppz]^{2+}$ photoluminescence in H4 and H4/α-syn-GFP cells. Cells were incubated with a range of $[Ru(phen)_2dppz]^{2+}$ concentrations, and $[Ru(phen)_2dppz]^{2+}$ photoluminescence intensity was quantified by flow cytometry. As expected, untreated H4 cells (that do not overexpress αS) did not display significant $[Ru(phen)_2dppz]^{2+}$ photoluminescence. However, we did observe an increase in $[Ru(phen)_2dppz]^{2+}$ photoluminescence signal in H4 cells overexpressing αS (H4/α-syn-GFP; Figure 2a). MG-132, an inhibitor of proteasomal degradation,[47] was used to induce aggregation of misfolding-prone proteins, including αS.[44] MG-132 treatment resulted in dramatic increase in $[Ru(phen)_2dppz]^{2+}$ photoluminescence in H4 cells suggesting that $[Ru(phen)_2dppz]^{2+}$ binds to protein aggregates, since a reasonable percentage of proteins are aggregation-prone[18,48] and MG-132 treatment promotes aggregation.[49] The increase in $[Ru(phen)_2dppz]^{2+}$ photoluminescence was even more dramatic when MG-132 treatment was applied to H4/α-syn-GFP cells, which is expected to cause accumulation of αS aggregates. Similarly to what we discussed for the $[Ru(phen)_2dppz]^{2+}$ in the presence of αS aggregates, we hypothesized that the changes in photoluminescence due to protein aggregation in H4 cells treated with MG-132 are a

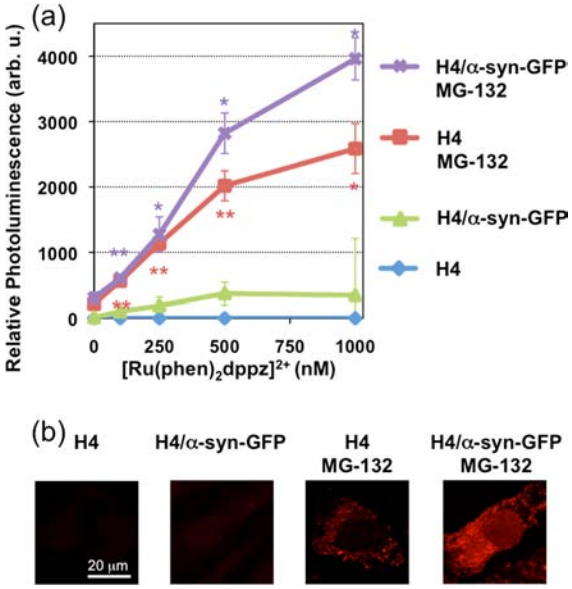

Figure 2. $[Ru(phen)_2dppz]^{2+}$ photoluminescence intensity in H4 and H4/α-syn-GFP cells. Flow cytometry analysis of $[Ru(phen)_2dppz]^{2+}$ photoluminescence intensity in H4 and H4/α-syn-GFP cells untreated and treated with MG-132 (2 μM) for 16 h (*$p < 0.05$, **$p < 0.005$). $[Ru(phen)_2dppz]^{2+}$ photoluminescence was measured using a 488 nm laser and a 585/42 band-pass filter. The relative photoluminescence was calculated by subtracting the background photoluminescence of $[Ru(phen)_2dppz]^{2+}$ in untreated H4 cells. The experiments were repeated three times, and the data are reported as mean ± SD.

dx.doi.org/10.1021/ja3100287 | J. Am. Chem. Soc. 2012, 134, 20776−20782

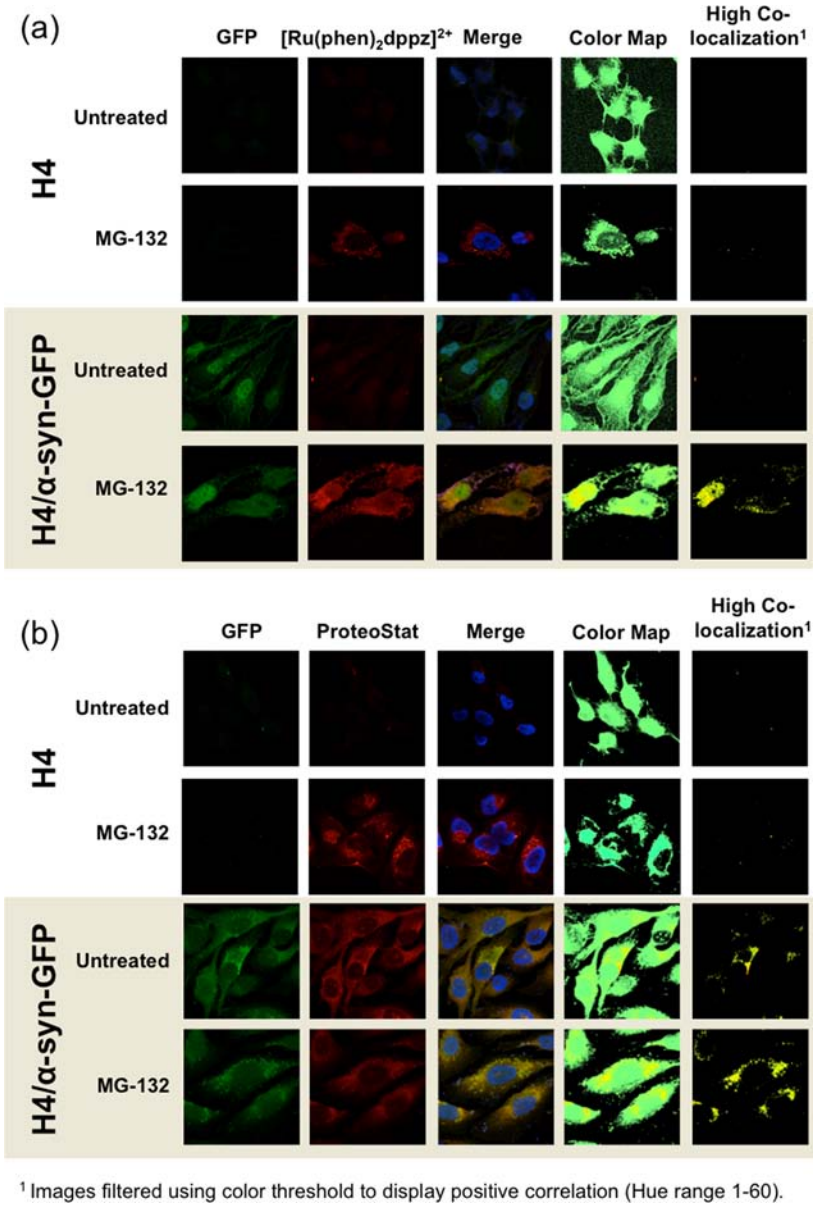

Figure 3. Detection of αS aggregation in H4 and H4/α-syn-GFP cells. Fluorescence microscopy images of H4 and H4/α-syn-GFP cells untreated and treated with MG-132 (2 μM) for 16 h. Aggregation was detected using $[Ru(phen)_2dppz]^{2+}$ (a) or ProteoStat dye (b). Images of α-syn-GFP fluorescence (green, column 1) and aggregates (red, column 2) were merged (column 3) and analyzed using NIH ImageJ software. Colocalization of GFP and $[Ru(phen)_2dppz]^{2+}$ or ProteoStat dye were evaluated using the Colocalization Colormap plugin (column 4). High colocalization represented by hot colors was depicted by filtering colormap images based on hue as described in the Experimental Section (pixels 1−60) (column 5).

consequence of partially denatured structure of protein aggregates, which expose hydrophobic cavities where $[Ru(phen)_2dppz]^{2+}$ can bind. Binding of $[Ru(phen)_2dppz]^{2+}$ to these hydrophobic sites would favor the excited-state population of "bright state" over the energetically favorable "dark state" of these ruthenium complexes in aqueous solution.[50]

To determine the optimal $[Ru(phen)_2dppz]^{2+}$ concentration that leads to minimal nonspecific binding and background photoluminescence, we analyzed microscopy images of H4 and H4/α-syn-GFP cells treated with $[Ru(phen)_2dppz]^{2+}$ under the same conditions. Representative images (0.5 μM $[Ru(phen)_2dppz]^{2+}$) are reported in Figure 2b and confirmed the results obtained by flow cytometry. Interestingly, in MG-132 treated cells, the aggregates detected with $[Ru(phen)_2dppz]^{2+}$ are granular and dispersed throughout the cell.

To demonstrate that the $[Ru(phen)_2dppz]^{2+}$ photoluminescence observed under conditions that promote aggregation of cellular proteins in H4/ αS-GFP cells is in great part due to $[Ru(phen)_2dppz]^{2+}$ binding to αS aggregates, we evaluated colocalization of GFP fluorescence and $[Ru(phen)_2dppz]^{2+}$ photoluminescence in H4 and H4/α-syn-GFP cells. Fluorescence microscopy images of H4 and H4/α-syn-GFP cells incubated with the optimal $[Ru(phen)_2dppz]^{2+}$ concentration (0.5 μM) (Figure 3, columns 1 and 2) were merged and quantified using the ImageJ script Colocalization Colormap (as described in the Experimental Section). The results are presented as a colocalization colormap, where "hot" colors represent a positive correlation and "cold" colors represent a

dx.doi.org/10.1021/ja3100287 | J. Am. Chem. Soc. 2012, 134, 20776−20782

negative correlation (Figure 2, column 4).[34] Colocalization colormaps were then filtered using a color threshold script in ImageJ to display only pixels with positive correlation (Figure 3, column 5). High $[Ru(phen)_2dppz]^{2+}$ photoluminescence signal, which colocalized with αS-GFP as indicated by the hot colors in the filtered colocalization colormaps (high colocalization, column 5) was detected in H4/α-syn-GFP cells treated with MG-132. Control studies demonstrated that GFP fluorescence is not observed in the channel used to detect $[Ru(phen)_2dppz]^{2+}$ photoluminescence (Figure S4), suggesting that the emission spectrum of GFP and $[Ru(phen)_2dppz]^{2+}$ do not overlap and $[Ru(phen)_2dppz]^{2+}$ can be utilized in the presence of other commonly used green fluorescent reporters.

To further evaluate the use of $[Ru(phen)_2dppz]^{2+}$ to detect aggregation in cell cultures, we compared it to the commercially available ProteoStat dye, a 488 nm excitable red fluorescent molecule that specifically interacts with denatured proteins within protein aggregates.[49] Similar to what we reported using $[Ru(phen)_2dppz]^{2+}$ above, we observed binding of the ProteoStat dye under conditions that promote protein aggregation (e.g., proteasome inhibition and overexpression of αS-GFP) (Figure 3b). The higher apparent binding of ProteoStat dye than $[Ru(phen)_2dppz]^{2+}$ and higher colocalization with αS-GFP in untreated H4/α-syn-GFP cells are likely due to different affinities of these molecules for αS and to different photoluminescence properties of the dyes.

To quantify $[Ru(phen)_2dppz]^{2+}$ binding to aggregated proteins, we calculated the aggregation propensity factor (APF, calculated as described in the Experimental Section) of H4 and H4/α-syn-GFP cells treated with MG-132 relative to untreated H4 cells. Cells were treated with MG-132 and binding of $[Ru(phen)_2dppz]^{2+}$ (0.5 μM) or ProteoStat dye (1:14,000 dilution) was measured by flow cytometry. In samples treated with $[Ru(phen)_2dppz]^{2+}$, the APF of H4 cells treated with MG-132 was 54.8% compared to untreated H4 cells (Figure 4). H4/α-syn-GFP cells displayed an APF of 12.3, which was further enhanced to 58.2% upon MG-132 treatment. In cells treated with ProteoStat dye, reported here for comparison, MG-132 treatment resulted in a dramatic increase in APF in H4 cells (70.5%) and in H4/α-syn-GFP cells (from 30.9% in untreated cells to 58.7% in MG-132 treated cells), which is similar to what is observed using $[Ru(phen)_2dppz]^{2+}$. These findings confirm the results obtained with fluorescence microscopy and demonstrate the use of $[Ru(phen)_2dppz]^{2+}$ as a molecular probe to monitor protein aggregation in cell culture.

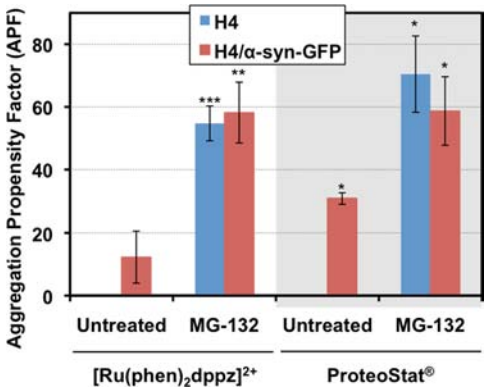

Figure 4. Aggregation propensity factor (APF) of H4 and H4/α-syn-GFP cells. H4 and H4/α-syn-GFP cells untreated and treated with MG-132 (2 μM) for 16 h were stained with $[Ru(phen)_2dppz]^{2+}$ (0.5 μM) or ProteoStat dye (*p < 0.05, **p < 0.01, ***p < 0.005), and photoluminescence was monitored by flow cytometry. The aggregation propensity factor (APF) was calculated using the following formula: $APF = 100(MFI_{treated} - MFI_{control})/MFI_{treated}$ where MFI is the mean photoluminescence intensity, and untreated H4 cells were used as the control. The experiments were repeated three times, and data are reported as mean ± SD.

CONCLUSIONS

A number of chemical properties of metal complexes including long lifetimes, photostability, large Stokes shifts, and red emission make these compounds an attractive alternative to more widely used organic dyes. Moreover, their large Stokes shift will allow their simultaneous use with other fluorescent probes emitting in the blue and green spectral regions. In summary, we report here that $[Ru(phen)_2dppz]^{2+}$ can be used to monitor real-time formation of αS fibril aggregates. Furthermore, $[Ru(phen)_2dppz]^{2+}$ was used to probe the presence of αS aggregates in an *in vitro* model of PD. $[Ru(phen)_2dppz]^{2+}$ photoluminescence signal was shown to correlate with the amount of cellular aggregates and to respond to modulation of the protein quality control system achieved via inhibition of proteasomal degradation (Figures 2–4). $[Ru(phen)_2dppz]^{2+}$ photoluminescence was also quantified by flow cytometry, paving the way for applications of this novel, highly sensitive molecular probe in high-throughput screens for the discovery of therapeutic targets for PD. In summary, this study provides a proof-of-principle demonstration of the use of ruthenium(II) dipyridophenazine complexes to monitor aggregation of amyloidogenic proteins *in vitro*. Results from this study open the way to more detailed investigations of the unique photoluminescence properties of this diverse class of metal compounds, enabling their use to study protein misfolding diseases and develop therapeutic strategies to prevent the aberrant accumulation of proteinaceous aggregates.

ASSOCIATED CONTENT

Supporting Information

Absorption and emission spectra of dipyridophenazine ruthenium(II) complexes, *in vitro* detection of A30P αS fibrils using $[Ru(phen)_2dppz]^{2+}$, comparison of the photoluminescence intensity of BSA and $[Ru(phen)_2dppz]^{2+}$, and microscopy of H4 and H4/α-syn-GFP cells without $[Ru(phen)_2dppz]^{2+}$. This material is available free of charge via the Internet at http://pubs.acs.org.

AUTHOR INFORMATION

Corresponding Author

segatori@rice.edu; amarti@rice.edu

Author Contributions

⊥These authors contributed equally.

Notes

The authors declare no competing financial interest.

ACKNOWLEDGMENTS

We thank the Welch foundation (C-1743 to A.A.M.) and the NSF (CBET-1159640 to LS and 0940902 to K.K.) for financial support. We also thank Prof. David Sulzer for generously providing A30P protein.

REFERENCES

(1) Dauer, W.; Przedborski, S. *Neuron* **2003**, *39*, 889–909.

(2) Spillantini, M. G.; Schmidt, M. L.; Lee, V. M. Y.; Trojanowski, J. Q.; Jakes, R.; Goedert, M. *Nature* **1997**, *388*, 839−840.
(3) Uversky, V. N. *Curr. Protein Pept. Sci.* **2008**, *9*, 507−540.
(4) Baba, M.; Nakajo, S.; Tu, P. H.; Tomita, T.; Nakaya, K.; Lee, V. M. Y.; Trojanowski, J. Q.; Iwatsubo, T. *Am. J. Pathol.* **1998**, *152*, 879−884.
(5) Goedert, M. *Nat. Rev. Neurosci.* **2001**, *2*, 492−501.
(6) Fink, A. L. *Acc. Chem. Res.* **2006**, *39*, 628−634.
(7) Morris, A. M.; Watzky, M. A.; Finke, R. G. *Biochim. Biophys. Acta, Proteins Proteomics* **2009**, *1794*, 375−397.
(8) Fortin, D. L.; Nemani, V. M.; Voglmaier, S. M.; Anthony, M. D.; Ryan, T. A.; Edwards, R. H. *J. Neurosci.* **2005**, *25*, 10913−10921.
(9) Roberti, M. J.; Jovin, T. M.; Jares-Erijman, E. *PLoS ONE* **2011**, *6*, e23338.
(10) Luk, K. C.; Hyde, E. G.; Trojanowski, J. Q.; Lee, V. M. Y. *Biochemistry* **2007**, *46*, 12522−12529.
(11) Antony, T.; Hoyer, W.; Cherny, D.; Heim, G.; Jovin, T. M.; Subramaniam, V. *J. Biol. Chem.* **2003**, *278*, 3235−3240.
(12) Biancalana, M.; Koide, S. *Biochim. Biophys. Acta, Proteins Proteomics* **2010**, *1804*, 1405−1412.
(13) Conway, K. A.; Harper, J. D.; Lansbury, P. T. *Biochemistry* **2000**, *39*, 2552−2563.
(14) Conway, K. A.; Harper, J. D.; Lansbury, P. T. *Nat. Med.* **1998**, *4*, 1318−1320.
(15) Viegas, M. S.; Martins, T. C.; Seco, F.; do Carmo, A. *Eur. J. Histochem.* **2007**, *51*, 59−66.
(16) Viegas, M. S.; M., T.; Seco, F.; do Carmo, A. *Eur. J. Histochem.* **2009**, *51*, 59−66.
(17) Hudson, S. A.; Ecroyd, H.; Kee, T. W.; Carver, J. A. *FEBS J.* **2009**, *276*, 5960−5972.
(18) Dobson, C. M. *Nature* **2003**, *426*, 884−890.
(19) Friedman, A. E.; Chambron, J. C.; Sauvage, J. P.; Turro, N. J.; Barton, J. K. *J. Am. Chem. Soc.* **1990**, *112*, 4960−4962.
(20) Cook, N. P.; Torres, V.; Jain, D.; Martí, A. A. *J. Am. Chem. Soc.* **2011**, *133*, 11121−11123.
(21) Erkkila, K. E.; Odom, D. T.; Barton, J. K. *Chem. Rev.* **1999**, *99*, 2777−2796.
(22) Boon, E. M.; Barton, J. K. *Curr. Opin. Struct. Biol.* **2002**, *12*, 320−329.
(23) Jain, D.; Saha, A.; Marti, A. A. *Chem. Commun.* **2011**, *47*, 2246−2248.
(24) Puckett, C. A.; Barton, J. K. *Biochemistry* **2008**, *47*, 11711−11716.
(25) Puckett, C. A.; Barton, J. K. *J. Am. Chem. Soc.* **2006**, *129*, 46−47.
(26) Gill, M. R.; Thomas, J. A. *Chem. Soc. Rev.* **2012**, *41*, 3179−3192.
(27) Fernandez-Moreira, V.; Thorp-Greenwood, F. L.; Coogan, M. P. *Chem. Commun.* **2010**, *46*, 186−202.
(28) Thorp-Greenwood, F. L. *Organometallics* **2012**, *31*, 5685−5692.
(29) Jenkins, Y.; Friedman, A. E.; Turro, N. J.; Barton, J. K. *Biochemistry* **1992**, *31*, 10809−10816.
(30) Sullivan, B. P.; Salmon, D. J.; Meyer, T. J. *Inorg. Chem.* **1978**, *17*, 3334−3341.
(31) Dickeson, J.; Summers, L. *Aust. J. Chem.* **1970**, *23*, 1023−1027.
(32) Amouyal, E.; Homsi, A.; Chambron, J.-C.; Sauvage, J.-P. *J. Chem. Soc., Dalton Trans.* **1990**, 1841−1845.
(33) Hiort, C.; Lincoln, P.; Norden, B. *J. Am. Chem. Soc.* **1993**, *115*, 3448−3454.
(34) Jaskolski, F.; Mulle, C.; Manzoni, O. J. *J. Neurosci. Methods* **2005**, *146*, 42−49.
(35) Uversky, V. N. *Curr. Protein Peptide Sci.* **2008**, *9*, 507−540.
(36) Although the determination of Stokes shifts for ruthenium metal complexes is not trivial, we will use this term throughout the manuscript as the difference between the maximum of the lowest-lying MLCT band in the absorption spectrum and the maximum in the photoluminescence spectrum.
(37) Kruger, R.; Kuhn, W.; Muller, T.; Woitalla, D.; Graeber, M.; Kosel, S.; Przuntek, H.; Epplen, J. T.; Schols, L.; Riess, O. *Nat. Genet.* **1998**, *18*, 106−108.
(38) Polymeropoulos, M. H.; Lavedan, C.; Leroy, E.; Ide, S. E.; Dehejia, A.; Dutra, A.; Pike, B.; Root, H.; Rubenstein, J.; Boyer, R.; Stenroos, E. S.; Chandrasekharappa, S.; Athanassiadou, A.; Papapetropoulos, T.; Johnson, W. G.; Lazzarini, A. M.; Duvoisin, R. C.; DiIorio, G.; Golbe, L. I.; Nussbaum, R. L. *Science* **1997**, *276*, 2045−2047.
(39) Li, J.; Uversky, V. N.; Fink, A. L. *Biochemistry* **2001**, *40*, 11604−11613.
(40) Zarranz, J. J.; Alegre, J.; Gomez-Esteban, J. C.; Lezcano, E.; Ros, R.; Ampuero, I.; Vidal, L.; Hoenicka, J.; Rodriguez, O.; Atares, B.; Llorens, V.; Tortosa, E. G.; del Ser, T.; Munoz, D. G.; de Yebenes, J. G. *Ann. Neurol.* **2004**, *55*, 164−173.
(41) Conway, K. A.; Lee, S. J.; Rochet, J. C.; Ding, T. T.; Williamson, R. E.; Lansbury, P. T. *Proc. Natl. Acad. Sci. U. S. A.* **2000**, *97*, 571−576.
(42) Walsh, D. M.; Lomakin, A.; Benedek, G. B.; Condron, M. M.; Teplow, D. B. *J. Biol. Chem.* **1997**, *272*, 22364−22372.
(43) Real-time fibrillization assays for α-synuclein with ThT performed by Antony et al. (Antony, T.; Hoyer, W.; Cherny, D.; Heim, G.; Jovin, T. M.; Subramaniam, V. *J. Biol. Chem.* **2003**, *278*, 3235−3240) showed lag and saturation times of 2 and 9 h respectively (100 μM spermine, 70 μM α-synuclein). Our experiments, which were conducted under similar conditions (100 μM spermine, 100 μM α-synuclein), show almost identical curves with lag and saturation times of 1.6 and 8.3 h, respectively. The slightly shorter times could be due to experimental variability or, more likely, to the slightly higher concentration of α-synuclein used in our experiments.
(44) McLean, P. J.; Kawamata, H.; Hyman, B. T. *Neuroscience* **2001**, *104*, 901−912.
(45) Pandey, N.; Schmidt, R. E.; Galvin, J. E. *Exp. Neurol.* **2006**, *197*, 515−520.
(46) Schwach, G.; Tschemmernegg, M.; Pfragner, R.; Ingolic, E.; Schreiner, E.; Windisch, M. *J. Mol. Neurosci.* **2010**, *41*, 80−88.
(47) Huang, L.; Chen, C. H. *Curr. Med. Chem.* **2009**, *16*, 931−939.
(48) David, D. C.; Ollikainen, N.; Trinidad, J. C.; Cary, M. P.; Burlingame, A. L.; Kenyon, C. *PLoS Biol* **2010**, *8* (8), e1000450.
(49) Shen, D.; Coleman, J.; Chan, E.; Nicholson, T. P.; Dai, L.; Sheppard, P. W.; Patton, W. F. *Cell Biochem. Biophys.* **2011**, *60*, 173−185.
(50) Brennaman, M. K.; Alstrum-Acevedo, J. H.; Fleming, C. N.; Jang, P.; Meyer, T. J.; Papanikolas, J. M. *J. Am. Chem. Soc.* **2002**, *124*, 15094−15098.